Pulse Profiles, Accretion Column Dips and a Flare in GX 1+4 During a Faint State

A. B. Giles[1,2,3], D. K. Galloway[1,4], J. G. Greenhill[1], M. C. Storey[1], C. A. Wilson[5]

[1] School of Mathematics and Physics

University of Tasmania

GPO Box 252-21, Hobart

Tasmania 7001, Australia

[2] *also* Laboratory for High Energy Astrophysics

Mail Code 662, NASA Goddard Space Flight Center

Greenbelt, MD 20771, USA

[3] *also* Universities Space Research Association

[4] Special Research Centre for Theoretical Astrophysics

School of Physics, University of Sydney

Sydney, NSW 2006, Australia

[5] Space Science Laboratory

NASA Marshall Space Flight Center

Huntsville, AL 35812, USA

Received ______________________; accepted ______________________

ABSTRACT

The *Rossi X-ray Timing Explorer* (RXTE) spacecraft observed the X-ray pulsar GX 1+4 for a period of 34 hours on July 19/20 1996. The source faded from an intensity of $\sim$ 20 mcrab to a minimum of $\leq$ 0.7 mcrab and then partially recovered towards the end of the observation. This extended minimum lasted $\sim$40,000 seconds. Phase folded light curves at a barycentric rotation period of 124.36568 $\pm$ 0.00020 seconds show that near the center of the extended minimum the source stopped pulsing in the traditional sense but retained a weak dip feature at the rotation period. Away from the extended minimum the dips are progressively narrower at higher energies and may be interpreted as obscurations or eclipses of the hot spot by the accretion column. The pulse profile changed from leading-edge bright before the extended minimum to trailing-edge bright after it. Data from the *Burst and Transient Source Experiment* (BATSE) show that a torque reversal occurred < 10 days after our observation. Our data indicate that the observed rotation departs from a constant period with a $\dot{P}/P$ value of $\sim -1.5\%$ per year at a 4.5σ significance. We infer that we may have serendipitously obtained data, with high sensitivity and temporal resolution about the time of an accretion disk spin reversal. We also observed a rapid flare which had some precursor activity, close to the center of the extended minimum.

Subject headings: Accretion; eclipses - Pulsars: individual (GX 1+4) - Stars: neutron - X-Rays: stars

1. INTRODUCTION

The binary X-ray pulsar GX 1+4 is unique in many respects. It is the only known hard X-ray source in a symbiotic system. Its optical companion is V2116 Oph, a 19th magnitude M6 III giant. It has the largest known rate of change of pulse period, with $\dot{P}/P$ as high as 2% per year in the 1970's. The relationship between the spin period history and the luminosity is much more complex than is predicted by standard accretion theory (Ghosh & Lamb 1979), with sustained periods observed where the spin-down rate was /it inversely /tm correlated with X-ray flux (Chakrabarty et al. 1997). Furthermore, GX 1+4 is thought to have a magnetic field of $\sim 3 \times 10^{13}$ Gauss (Dotani et al. 1989; Greenhill et al. 1993; Cui 1997) which is amongst the strongest known for any object.

The mean X-ray flux from GX 1+4 is variable on timescales of days to decades. In the decade following its discovery in 1971 (Lewin, Ricker & McClintock 1971) the flux was persistently high at > 100 mcrab (McClintock & Leventhal 1989). During the early 1980's the flux decreased by several orders of magnitude (to < 0.5 mcrab on one occasion, Mukai 1988) and since then the source has normally been toward the lower end of its historical intensity range. There is considerable uncertainty about the source distance of 3 - 15 kpc (Chakrabarty & Roche 1997) and hence about the X-ray luminosity. The very long-term flux variations are correlated with both spin period history and pulse profiles. During the 1970s when the pulsar was spinning up steadily the typical pulse profiles in most energy bands were broad, brighter on the trailing-edge and sometimes with a secondary minimum (see e.g. Doty, Hoffman & Lewin 1981). With the change to a lower flux state in the 1980s the pulsar began steady spin-down (with brief returns to spin-up) and the observed pulse profiles were typically leading-edge bright (Greenhill, Galloway & Storey 1998). The orbital period is unknown but is thought to be of the order of one year (Cutler et al. 1986).

2. THE OBSERVATIONS

The *Rossi X-ray Timing Explorer* (RXTE) observed GX 1+4 for a useable total of 51,360 seconds during a ~34 hour period starting at 16:46 UT on 19th July 1996. The observations were made in 23 sections with the interruptions being due to regular passages through the South Atlantic Anomaly (SAA) and Earth occultations of the source. Five additional short gaps were due to RXTE monitoring campaigns on other sources. The variation in intensity seen by the Proportional Counter Array (PCA) detectors (Zhang et al. 1993) is shown in the upper panel of Fig. 1. The data are shown for Proportional Counter Units (PCU's) 1, 2 & 3 since PCU 4 was turned off after 0:03 UT on 20th July and PCU 5 after 2:32 UT on 20th July. These two detectors are occasionally commanded off to provide high voltage rest periods. Throughout this paper all analysis results and figures apply to the summation of PCU's 1, 2 & 3 only, all the data have been background subtracted and all quoted UT values are barycentric times. The principal observing mode used was E_250US_128M_0_8S and so every detected X-ray photon was time tagged to 250μs and its energy was measured in 128 pulse height channels.

These RXTE observations were proposed with the particular intention of studying the high energy spectrum of GX1+4. However, the source turned out to be much weaker than expected in all energy bands so, in this paper we do not discuss any data from the High Energy X-ray Timing Experiment (HEXTE) on RXTE. Since the source was relatively faint the PCA background subtraction becomes critical. We have used the RXTE guest observers PCABACKEST software to estimate the various instrumental and orbital background contributions. The background model used was "sky VLE". Due to the proximity of GX 1+4 to the galactic plane we have also subtracted a 'galactic ridge' emission component determined from data in Valinia & Marshall (1998). Their results were used to calculate integrated count rates in the direction of GX 1+4 for our light curve energy ranges of 2 -

7 keV & 7 - 20 keV. The derived rates were also compared to the PCA count rates seen in the vicinity of GX 1+4 for the various slews to and from the source which were made during our observation. For the 2 - 7 keV range we have taken a value of 3.46 counts s^{-1} and for the 7 - 20 keV range 0.64 counts s^{-1}. We estimate that any remaining systematic error in our background subtraction is ~ 0.5 counts s^{-1}.

We do not discuss any spectral analysis results in this paper since our primary concern here is with timing issues. We do, however, see clear spectral variations with pulse phase and a full presentation of the phase resolved spectral analysis can be found in Galloway et al. (1999) which also discusses the spectral evolution through the flare reported here.

3. TEMPORAL STUDIES

During the observation the flux decreased to a minimum after about 20 hours and then began a gradual recovery towards its initial intensity. The light curve is shown in the upper panel of Fig. 1 and is plotted as a 4 second running average with a time resolution of one second. The Crab produces ~7,800 counts s^{-1} in 3 PCU's so the source flux during this observation ranges from ≤ 0.7 to ~ 20 mcrab. We have divided the complete observation into the three intervals marked as 1 - 3 in Fig. 1. The ~124 second rotation modulation creates a wide scatter of points and during the lowest intensity state in Fig. 1 (interval 2) the minima appear to almost reach zero. For data which are not running mean averaged, as in Fig. 1, the one second bins can in fact sometimes go negative after background subtraction. The widely varying intensity falls within an envelope where the upper and lower edges are defined by the maxima and minima respectively of the rotation modulation (see Figs. 4 & 5). In the lower panel in Fig. 1 we show the mean count rate averaged over complete rotation cycles according to our ephemeris as defined in section 3.1. Rotation cycles that are, for any reason incomplete are omitted, leaving a total of 344 plotted points.

There is still a factor of $\sim$2 variation over timescales corresponding to tens of rotation cycles and the variability roughly scales with the intensity. We have fitted a Gaussian curve to these data points since the distribution appears to be symmetrical about the minimum. The center of the extended minimum is at UT 17:43:45 $\pm$ 50 seconds on 20th July 1996 with a σ width of 19467 $\pm$ 78 seconds. The initial level is not well defined but for the fit shown is 56.4 $\pm$ 0.1 counts s^{-1} with a minimum during interval 2 of 5.65 $\pm$ 0.2 counts s^{-1}. There is a suggestion of less variability on the climb out of the extended minima than during the entry into it.

3.1. PERIOD DETERMINATION

The most persistent feature (see Fig. 4) of the rotation modulation is a sharp "dip" with a phase width of $\sim$ 0.05. This can be identified in published profiles from many previous measurements and is evident in the mean pulse profile even at the lowest count rates during interval 2. We use it to define phase zero for the pulse cycle. The PCA data on GX 1+4 have sufficient sensitivity that even with only three PCUs operating most of the individual rotation dips can be seen throughout the observation except during the faintest part of the extended minimum. There is no difficulty in maintaining the cycle count across the many gaps evident in Fig. 1. Denoting the first dip observed as number 1, the last one seen is number 975. Of this set only 405 occurred during RXTE on source time. The relative distributions of the data in the 3 intervals in Fig. 1 can be summarised as follows. Interval 1 spans dips 1 - 632 with 259 of these being during on source time and potentially observable, interval 2 spans dips 633 - 771 with a total of 44 being potentially observable and interval 3 spans dips 772 - 975 with 102 being potentially observable. To preserve sufficient signal to noise for the dip profiles, the data were first binned up into 1 second samples for the energy range 2 - 20 keV. We then used an initial period estimate to define the expected positions of the centers of the 405 dips. Fits were then performed to a small data window of ± 5 bins centered at each expected dip position to produce a plot of the observed dip time minus the calculated time (O - C), assuming a constant period, against dip cycle number (N). Since the individual dips can be quite noisy, are variable in profile, may possibly move around slightly in time and also do not descend from or recover to a well defined intensity level, we have chosen to use a simple parabolic curve for the fitting function. The intention is to provide a consistent estimate of the time of minimum count rate for each individual dip. This restricted goal also prompted us to fit the dips in the 2 - 20 keV light curves without the background subtraction applied. This has the advantage that the error treatment in the curve fitting process is more valid since the count rates are much closer to a normal distribution without reaching low, poisson dominated values, at the bottom of each dip. The dip total was reduced to only 309 after rejection of poorly fitted dips and also excluding all dips within interval 2 where the mean count rate was very low and the dips hardly detectable. We propose in a later section that these dips may be caused by eclipses of the hot spot by the accretion column.

A plot of the O - C residuals against dip cycle number, as in Fig. 2, shows considerable scatter around the mean but repeated trials, based on the assumption that the period is constant, allow adjustment of the period to provide the best fit. The linear fit for the period gives a value of P = 124.36568 $\pm$ 0.00020 seconds. This fit is represented by the horizontal dotted line across the center of Fig. 2. Since there is a reasonable expectation of seeing a small change in $\dot{P}/P$ over the 34 hour span of the observations we have also fitted a 2nd order polynomial to the data which is shown by the solid curved trace in Fig. 2. The times of dip minima for this fit are given by T = [N $\times$ 124.36213 $\pm$ 0.00080] + [$N^2 \times$ 0.00000344 $\pm$ 0.00000075] seconds where N is the cycle count starting from zero at the first observed dip. These fits suggest that the period is not constant during the observation and indicate a value for $\dot{P}/P$ of $\sim -1.5\%$ per year. The departure from a constant period has a 4.5σ significance. The larger error bars tend to dominate in Fig. 2 but ~40% of the 309 points have a standard deviation of $\leq \pm$ 0.5 seconds. Because individual dip profiles are often well fitted by a minimum which is substantially displaced in time from the expected position (up to a few seconds) we have examined the series of O - C residuals for any periodic component. The data have many gaps and ~66% are missing so, after rejection of the poorly fitted dips, we have used the method described by Bopp et al. (1970). This has revealed no periodic trends in the O - C residuals so we conclude that the pulse dips move about, through a small range, in a random fashion. The distribution of the O - C residuals is approximately gaussian with a σ width of ~2.3 seconds which corresponds to ~ 7 degrees in rotation phase. We have also compared the results obtained by repeating the above analysis for ±4, ±6 & ±7 bins in addition to the presented case of ±5 bins. The smallest of these windows is rather short compared to the width of the dip features evident in Figs. 4 & 5 but for all these cases the inferred $\dot{P}/P$ values and errors are similar. Equivalent plots to Fig. 2 for these other cases also look similar, however, the individual O - C values are different in each case, though the spread is within the typical error bars. A plot of the O - C values for the ±5 bin case against those for the ±6 bin case has a correlation coefficient of 0.89 for 286 points. The scatter along the expected +1 slope has a σ of ±0.4 seconds.

Historically GX 1+4 has spent most of its time in a spin down state (see Figure 1 & 2, Chakrabarty et al. 1997). The *Burst and Transient Source Experiment* (BATSE) data points presented by Chakrabarty et al. (1997) for the long term period changes in GX 1+4 were derived over 5 day intervals but BATSE could not detect GX 1+4 for an extended period encompassing our observation due to its weak state. The BATSE data for this period, derived from 4 - 8 day intervals, are illustrated in Fig. 3 which shows the pulse period and $\dot{P}$ changes over a ~ 100 day interval. The first BATSE detections of GX 1+4 after our observation show that spin up commenced within 10 days of our observation and lasted for 15 - 20 days before spin down resumed.

3.2. PHASE FOLDED LIGHT CURVES

The pulsar period derived in the previous section was used to construct phase folded pulse profiles for the entire data set in several energy channels. For this analysis the period was assumed to have a constant value of 124.36568 seconds. These pulse profiles are presented in two energy ranges in Figs. 4 & 5, each of which has a curve for the intervals marked as 1, 2 & 3 in Fig. 1. The pulse profiles clearly changed substantially during the observations. The profile during the brightest state (interval 1) was similar to others measured during the 1980-90's low state with the leading-edge brightest. Pulsations almost disappeared (ignoring the sharp dips) during the lowest intensity state (interval 2) but were again observed strongly when the flux increased once more (interval 3). The pulse profile however had changed significantly since interval 1, and was similar to those profiles measured during the 1970s, with the trailing-edge brightest. This change mirrors that which occurred between the 1970s and 1980s (Greenhill et al. 1998) but over a very much shorter timescale and with the change in the opposite direction. We are not aware of any previous observation of similar pulse profile changes on such short timescales.

In Table 1 we present the results from fitting gaussian profiles about phase 0.0 to the six dips shown in Figs. 4 & 5. Defining the pre-dip level for the gaussian is somewhat problematic but we have chosen the 'shoulder' in the count rate just prior to each dip. One could also argue that the dips have a rather flat bottom during the extended minimum through interval 2 but the count rate at the center of the dip is very low and the statistics relatively poor. Within the errors all six dips occur at exactly the same phase. The principal feature in Table 1 is that the dips are much shorter in duration in the 7 - 20 keV band than in the 2 - 7 keV band. In Figs. 4 & 5 the three curves have been vertically displaced for clarity but it is clear that the bottom of the dips, for all intervals in both figures, are almost coincident in count rate. A second feature in Table 1 is that the dips are narrower in interval 2 than in intervals 1 or 3. This suggests that when the source is brighter the enhanced emission is observed at all phases except the center of the dip. It is possible, given the uncertainties of the PCA background subtraction process, that the flat bottom of the dips for interval 2 in Figs. 4 & 5 represents zero flux from GX 1+4.

3.3. FLARE

A significant flare is visible in Fig. 1 near the center of the extended minimum. The flare center is at 17:23:38 UT on 20th July 1996 which corresponds to a phase of 0.67 on our rotation ephemeris, defined so that phase 0.0 is the phase of the primary minimum. A phase of 0.67 is similar to the phase of the brightest part of the pulse when the intensity rose again in interval 3 and the pulses were seen to be trailing-edge bright. The flare is shown in more detail in Fig. 6. A smaller enhancement in emission is seen at 17:22:46 UT and may represent the leading part of a trailing-edge bright pulse profile. The main part of the flare has a duration of ~6 seconds, although it is sharply peaked, and is superimposed on a longer somewhat triangular profile enhancement that covers about half of the basic ~124 second rotation period. The flare is roughly symmetrical with no sign of the characteristic sharp rise and exponential decline shown by type I X-ray bursts from neutron stars. The flare occurs only 1207 seconds before the center of the extended broad minimum. The close proximity is remarkable given the width of the feature of > 40,000 seconds but this may be a coincidence. In the 2 - 20 keV energy range the peak count rate of the flare was ~98.6 counts s^{-1} although the running average shown in Fig. 6 reduces this to ~83.9 counts s^{-1}. The peak rate was not exceeded elsewhere during a window of ±6.25 hours centered on the event.

There is a possibility that the flare originates from another X-ray source in the PCA field of view and not from GX 1+4 itself. The five PCA detectors are not quite co-aligned and for sufficiently bright flares an estimate can be made of their position relative to the spacecraft pointing direction (see 4.2, Strohmayer et al. 1997). Unfortunately this is not possible in this case since PCU's 1, 2 & 3 are closely aligned and the count rate from the flare is too low to get meaningful.results by this method.

In Fig. 6 there is also a strong indication of a precursor mini flare in the preceding rotation cycle to that of the main flare. The time interval between the precursor mini flare and the main flare is estimated to be 140 - 150 seconds, which is significantly longer than the neutron star rotation period of 124 seconds. However, if the two enhancements at 17:22:46 UT and 17:23:38 UT are part of the same pulse profile, then the separation between the two flaring episodes is similar to the pulse period. Galloway et al. (1999) have suggested an alternative explanation with these flares being due to episodes of accretion resulting from successive orbits of a locally dense patch of matter in the accretion disk. The pre-flare structure seen here in GX 1+4 is somewhat reminiscent of some of the bursting activity seen in GRO J1744-28 (Giles et al. 1996).

4. DISCUSSION

The low X-ray intensity during our 1996 observation has uncovered several unexpected new features of GX 1+4. The mechanism behind the pulse profile change may be related to the cause of the much longer term changes observed between the high state of the 1970s and the lower state which has persisted until the present day (Greenhill et al. 1998). That a similar pulse profile change can take place on such short timescales may provide information on the underlying disk dynamics and the spinup-spindown behaviour of the system (Greenhill et al. 1999). The origin of the very sharp dips in Figs. 4 & 5 is somewhat enigmatic, partly because spectral changes over the observation make model fitting very difficult (Galloway 1999). The width of this dip feature decreases with increasing energy.

A similar trend of decreasing width with increasing energy is apparent (but not remarked upon) in Ginga data (Makishima et al. 1988). The dip feature is present in our data during all three intervals, even when the flux drops to its lowest level.

In general, models predicting pulse profiles in X-ray pulsars (Leahy & Li 1995; Mészáros & Nagel 1985) appear unable to reproduce such narrow dip features. Since the sharp dips are present in the pulse profiles for all energies up to $\sim$ 100 keV (White et al. 1983; Greenhill et al. 1998) the mechanism responsible for the dip must be effective over a very wide energy range. Similar sharp dips observed in profiles from other pulsars (Cemeljic & Bulik 1998; Reig & Roche 1999) have been attributed to eclipses of the emission region by the accretion stream. The optical depth for non-resonant Compton scattering, which is likely to be an important process in the column, will vary depending on the relative orientation of the column with respect to the observer. In particular the optical depth will reach a maximum at the closest approach of the line of sight to the magnetic field axis because the line of sight then passes through a larger slice of the accretion column. The additional scattering for this alignment will produce a corresponding dip in the pulse profile which can be moderately sharp over a range of different geometries (Galloway, 1999). Another possible cause of a sharp dip is resonant cyclotron absorption which has been discussed by Dotani et al. (1989) and Greenhill et al. (1993). For this absorption process the emission at frequency ν can be very efficiently absorbed by the accretion plasma when the local cyclotron energy in the accretion stream is the same as ν. The accretion column becomes wider with height above the polar cap as the field lines diverge and the frequency that is most effectively absorbed also decreases with height as the magnetic field decreases. The scattering region in the column, at a height corresponding to each particular frequency, is expected to extend over a greater area than the polar cap below it and so can completely cover this X-ray "hot spot" for a substantial range of viewing angles. Hence, the line of sight does not need to be very closely aligned with the magnetic field axis for a significant dip to be created. Additionally, this model predicts that the width of the dip minimum should decrease with increasing energy as is seen in the data presented in this paper. It seems feasible that both the processes described above may be operating simultaneously in producing the observed dip. A further, but less likely, possibility (Storey et al. 1998; Greenhill et al. 1998) is that the line of sight is closest to the magnetic axis at phase 0.5 and that the primary dip represents the edge of a very broad pulse centered at phase 0.5. The asymmetry in the pulse profile could then be caused by an asymmetry in the accretion flow onto the polar cap region. A model of this type does not however provide a simple explanation for the energy dependence of the dip width.

The results presented above show that we have observed GX 1+4 during a transition from leading-edge bright pulses to trailing-edge bright pulses. There is strong evidence that this was associated with a reversal of torque in GX 1+4 and possibly a change in accretion disk spin direction. This observation and the modelling of Greenhill et al. (1999) suggests that our understanding of the processes of torque transfer in accreting X-ray pulsars would greatly benefit from more detailed observations of GX 1+4 through a torque reversal period. The flare observed during the time of intensity minimum may also provide new insights into the mechanisms of mass transfer from the accretion disk to the neutron star if more examples can be observed. There is marginal evidence for wandering in the phases of the individual sharp dips but the count rates are too low to allow detailed study of any such effect. If present, this could be interpreted as evidence for wander in the position of the accretion column if the dips are due to absorbtion by accreting matter. The reality of this hypothetical wandering could be tested by analysing observations of GX 1+4 obtained while it was in a higher intensity state.

We thank the RXTE Science Operations Center planning and operations staff for successfully conducting these observations. We also thank Kinwah Wu for helpful advice.

Jean Swank for support and useful discussions and Keith Jahoda for comments on the PCA background.

Table 1: Averaged profile parameters for the dip features in Figs. 4 & 5

Interval	Parameter	2 - 7 keV	7 - 20 keV
1	Center (phase)	0.9997 ± 0.0011	1.0002 ± 0.0008
	Half Width (sec)	3.82 ± 0.18	2.78 ± 0.12
	Depth (c s^{-1})	16.07 ± 0.57	18.61 ± 0.63
	Minima (c s^{-1})	2.04 ± 0.69	3.87 ± 0.71
2	Center (phase)	1.0030 ± 0.0029	0.9996 ± 0.0018
	Half Width (sec)	2.49 ± 0.40	2.02 ± 0.25
	Depth (c s^{-1})	4.59 ± 0.61	6.42 ± 0.68
	Minima (c s^{-1})	-0.58 ± 0.65	-0.03 ± 0.72
3	Center (phase)	1.0036 ± 0.0020	1.0026 ± 0.0011
	Half Width (sec)	4.24 ± 0.35	2.77 ± 0.16
	Depth (c s^{-1})	8.80 ± 0.52	12.74 ± 0.58
	Minima (c s^{-1})	1.69 ± 0.64	3.29 ± 0.64

REFERENCES

Bopp, B.W., Evans, D.S., Laing, J.D., & Deeming, T.J., 1970, MNRAS, 147, 355

Cemeljic, M., & Bulik, T., 1998, AcA, 48, 65

Chakrabarty, D., & Roche, P., 1997, ApJ, 489, 254

Chakrabarty, D., Bildsten, L., Finger, M.H., Grunsfeld, J.M., Koh, D.T., Nelson, R.W., Prince, T.A., Vaughan, B.A., & Wilson R.B., 1997, ApJ, 481, L101

Cui, W., 1997, ApJ, 482, L163

Cutler, E.P., Dennis, B.R., & Dolan, J.F., 1986, ApJ, 300, 551

Dotani, T., Kii, T., Nagase, F., Makishima, K., Ohashi, T., Sakao, T., Koyama, K., & Tuohy, I.R., 1989, Publ. Astr. Soc Japan, 41, 427

Doty, J.P., Hoffman, J.A., & Lewin, W.H.G., 1981, ApJ, 243, 257

Galloway, D.K., Giles, A.B., Greenhill, J.G., & Storey, M.C., 1999, MNRAS, submitted

Galloway, D.K., 1999, in preparation

Ghosh, P., & Lamb, F.K., 1979, ApJ, 234, 296

Giles, A.B., Swank, J.H., Jahoda, K., Zhang, W., Strohmayer, T., Stark, M.J., & Morgan, E.H., 1996, ApJ, 469, L25

Greenhill, J.G., Sharma, D.P., Dieters, S.W.B., Sood, R.K., Waldron, L., & Storey, M.C., 1993, MNRAS, 260, 21

Greenhill, J.G., Galloway, D.K., & Storey, M.C., 1998, PASA, 15, 254

Greenhill, J.G., Galloway, D.K., & Murray, J.R., 1999, PASA, in press

Leahy, D.A., & Li, L., 1995, MNRAS, 277, 1177

Lewin, W.H.G., Ricker, G.R., & McClintock, J.E., 1971, ApJ, 169, L17

McClintock, J.E., & Leventhal, M., 1989, ApJ, 346, 143

Makishima, K., Ohashi, T., Sakao, T., Dotani, T., Inoue, H., Koyama, K., Makino, F., Mitsuda, K., Nagase, F., Thomas, H.D., Turner, M.J.L., Kii, T., & Tawara, Y., 1988, Nature, 33, 746

Mészáros, P., & Nagel, W., 1985, ApJ, 299, 138

Mukai, K., 1988, The 1988 Low State of GX 1+4, Mullard Space Sci. Lab. Rep.

Reig, P., & Roche, P., 1999, MNRAS, 306, 95

Storey, M.C., Greenhill, J.G., & Kotani, T., 1998, PASA, 15, 254

Strohmayer, T.E., Jahoda, K., Giles, A.B., & Lee, U., 1997, ApJ, 486, 355

Valinia, A., & Marshall, F.E., 1998, ApJ, 505, 134

White, N.E., Swank, J.H., & Holt, S.S., 1983, ApJ, 270, 711

Zhang, W., Giles, A.B., Jahoda, K., Soong, Y., Swank, J.H., & Morgan, E.H., 1993, in EUVE, X-Ray and Gamma-Ray Instrumentation for Astronomy IV, Proc., SPIE 2006, 324

This manuscript was prepared with the AAS LaTeX macros v4.0.

Figure Captions

Figure 1. The light curve of the ~34 hour observation of GX 1+4. The count rate shown is a running 4 second average, with a one second resolution, for the full energy range of the PCA (2 - 20 keV). The rapid intensity variation reflects the pulse amplitude of the ~124.4 second rotation period and this is superimposed on a broad dip in intensity down to a minimum level of ≤ 0.7 mcrab. The flare is visible near the center of this broad minimum. The lower panel plots mean count rates for individual complete rotation cycles and a Gaussian fit through these data points.

Figure 2. This plot shows the trend in the fits to the dip minima for the 974 cycles covered by the observation in Fig. 1. Located and fitted individual dip centers are plotted plus or minus with respect to an ephemeris period of 124.36568 seconds. The error bars on the O - C residuals are $\pm 1\sigma$. The horizontal dotted line is the best linear fit and the solid curved line is the best fit 2nd order polynomial. The lower dotted curve is for a $\dot{P}/P$ of 1.5% per year.

Figure 3. The BATSE data for GX1+4 over the period from 20 April 1996 to 25 August 1996. The RXTE observation, at HJD $\sim$ 2450285, is marked with the small square and occurs just before a brief interval of spin up commenced. The $\dot{P}$ axis in the lower part of the figure is in units of 10^{-8} s s^{-1}.

Figure 4. Phase folded light curves for the energy range 2 - 7 keV. The three traces correspond to intervals 1, 2 & 3 in Fig. 1. To differentiate the three profiles trace 1 has been offset vertically by 10.0 counts s^{-1} and trace 3 by 5.0 counts s^{-1}. The large rotation modulation has shifted character between traces 1 & 3 with the maximum flux occurring in the earlier part of the cycle for trace 1 and the latter part for trace 3.

Figure 5. Phase folded light curves similar to those in Fig. 4 but for the higher energy

range of 7 - 20 keV. Trace 1 has again been offset vertically by 10.0 counts s^{-1} and trace 3 by 5.0 counts s^{-1}. The change in character for traces 1 & 3 noted for Fig. 4 is repeated for this energy band. Fits to the dip profiles in Figs. 4 & 5 are given in Table 1 and the feature is clearly sharper at higher energies.

Figure 6. The flare seen during the extended minima of GX1+4. To emphasize this feature the 2 - 20 keV count rate is plotted as a running 4 second average with one second resolution. The vertical dotted lines mark the times of the predicted dip minima.

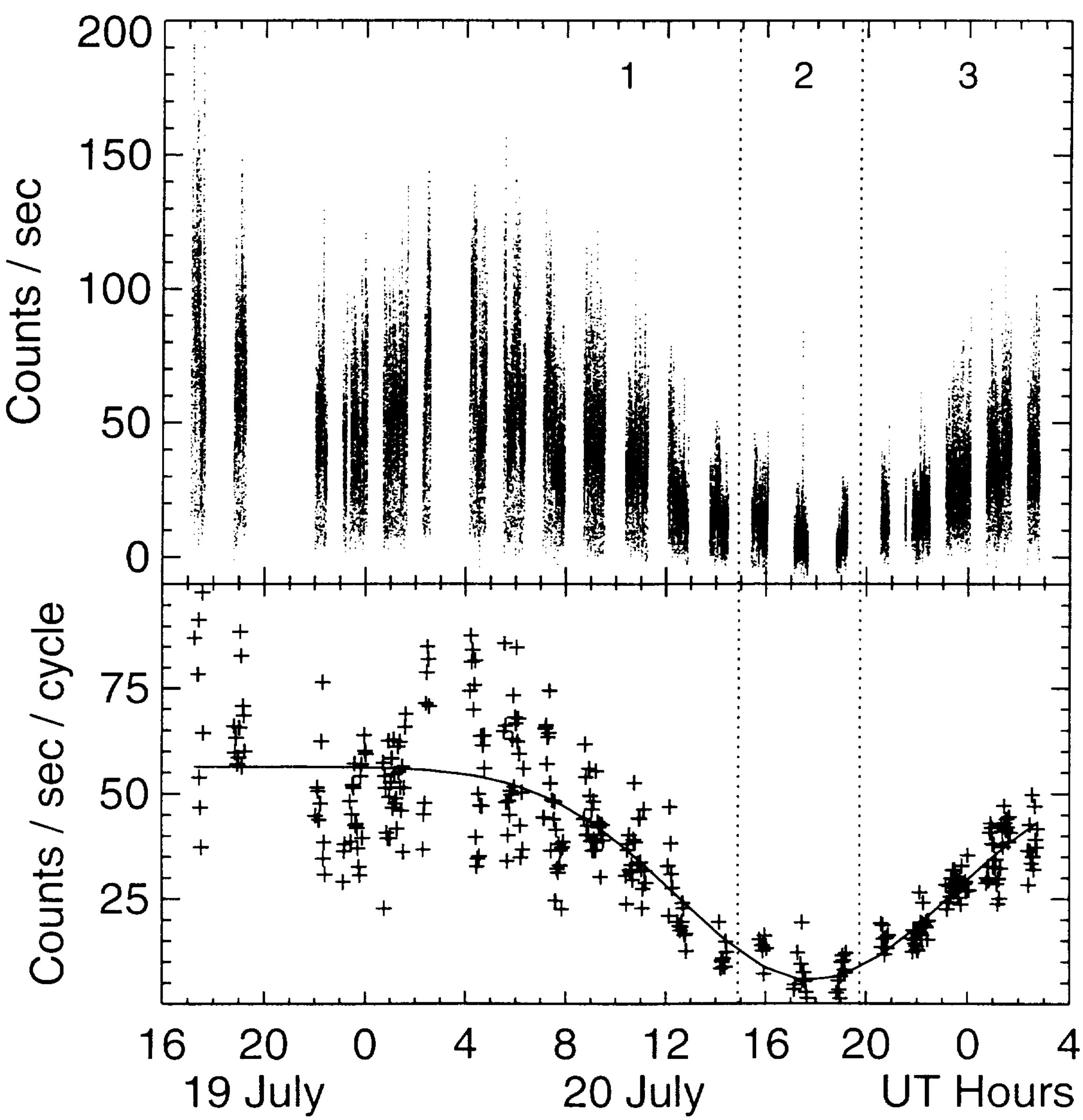

200
150
100
50
0
Counts / sec
1
2
3
75
50
25
Counts / sec / cycle
16
20
0
4
8
12
16
20
0
4
19 July
20 July
UT Hours

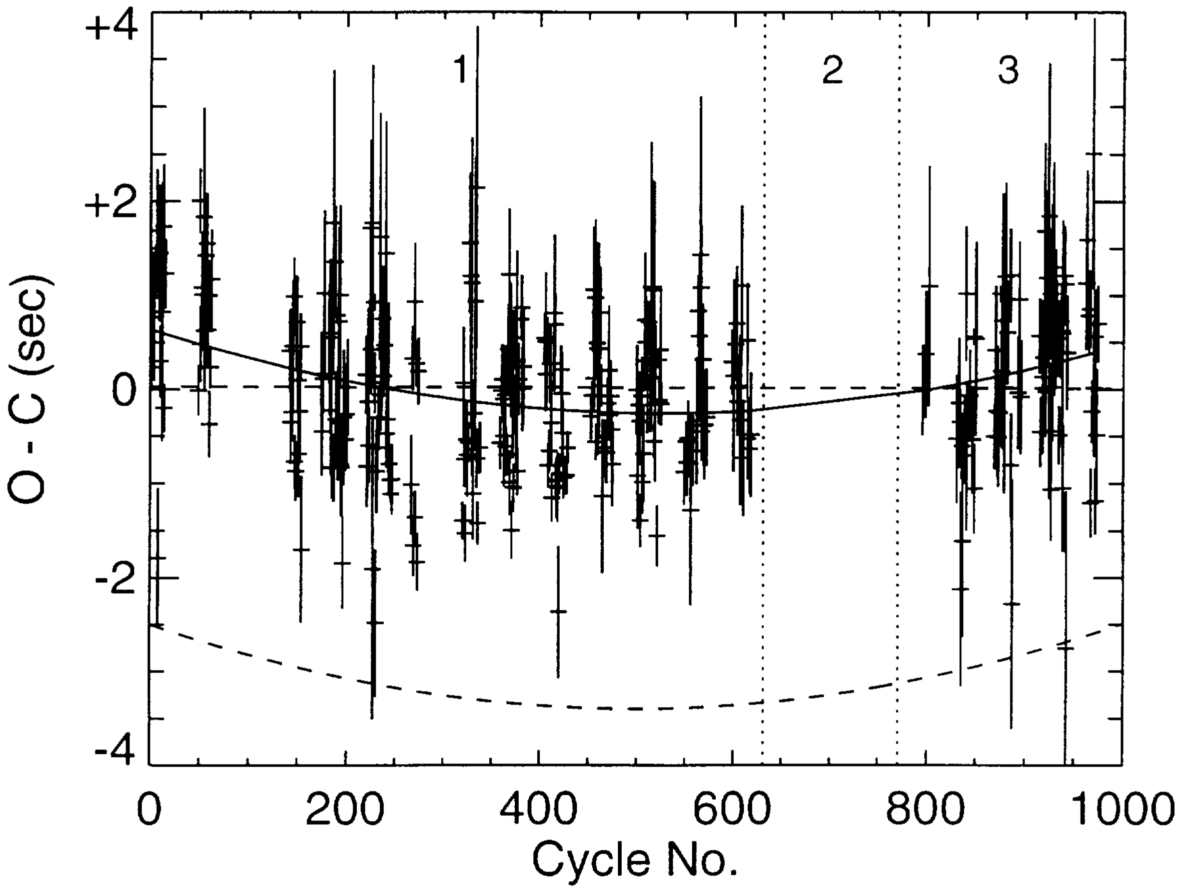

1
2
3
+4
+2
0
-2
-4
O - C (sec)
0
200
400
600
800
1000
Cycle No.

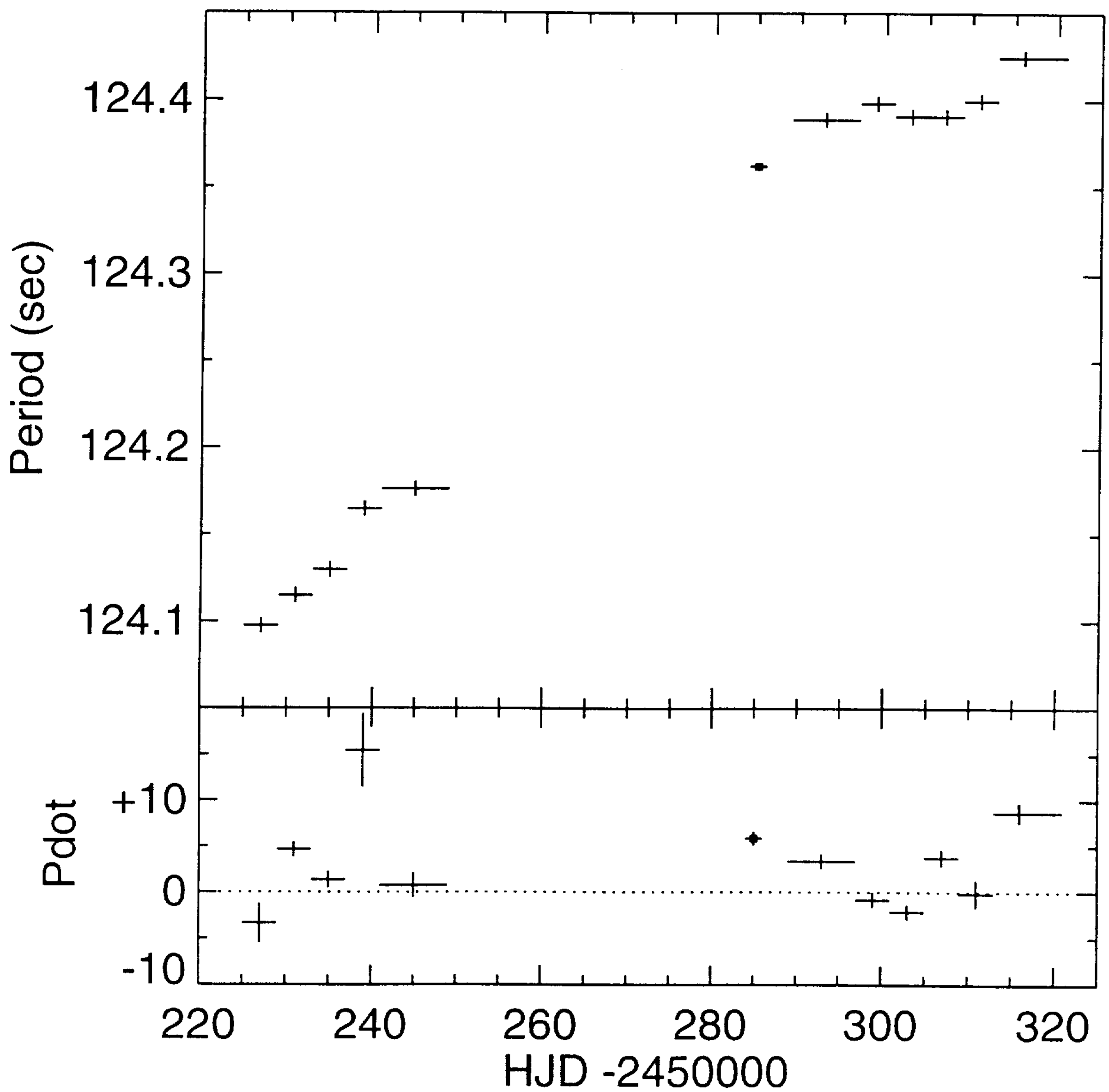

124.4
124.3
124.2
124.1
Period (sec)
+10
0
-10
Pdot
220
240
260
280
300
320
HJD -2450000

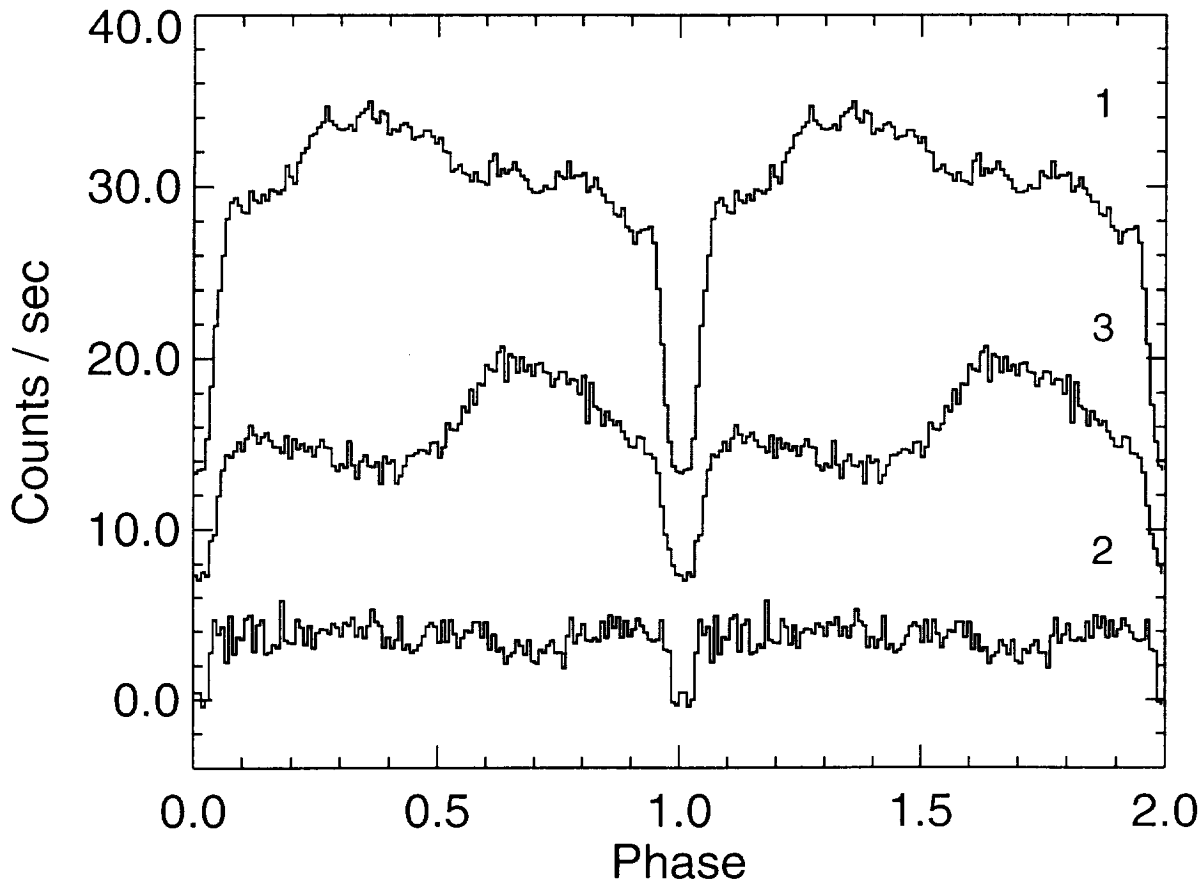
40.0
30.0
20.0
10.0
0.0
Counts / sec
1
3
2
0.0
0.5
1.0
1.5
2.0
Phase

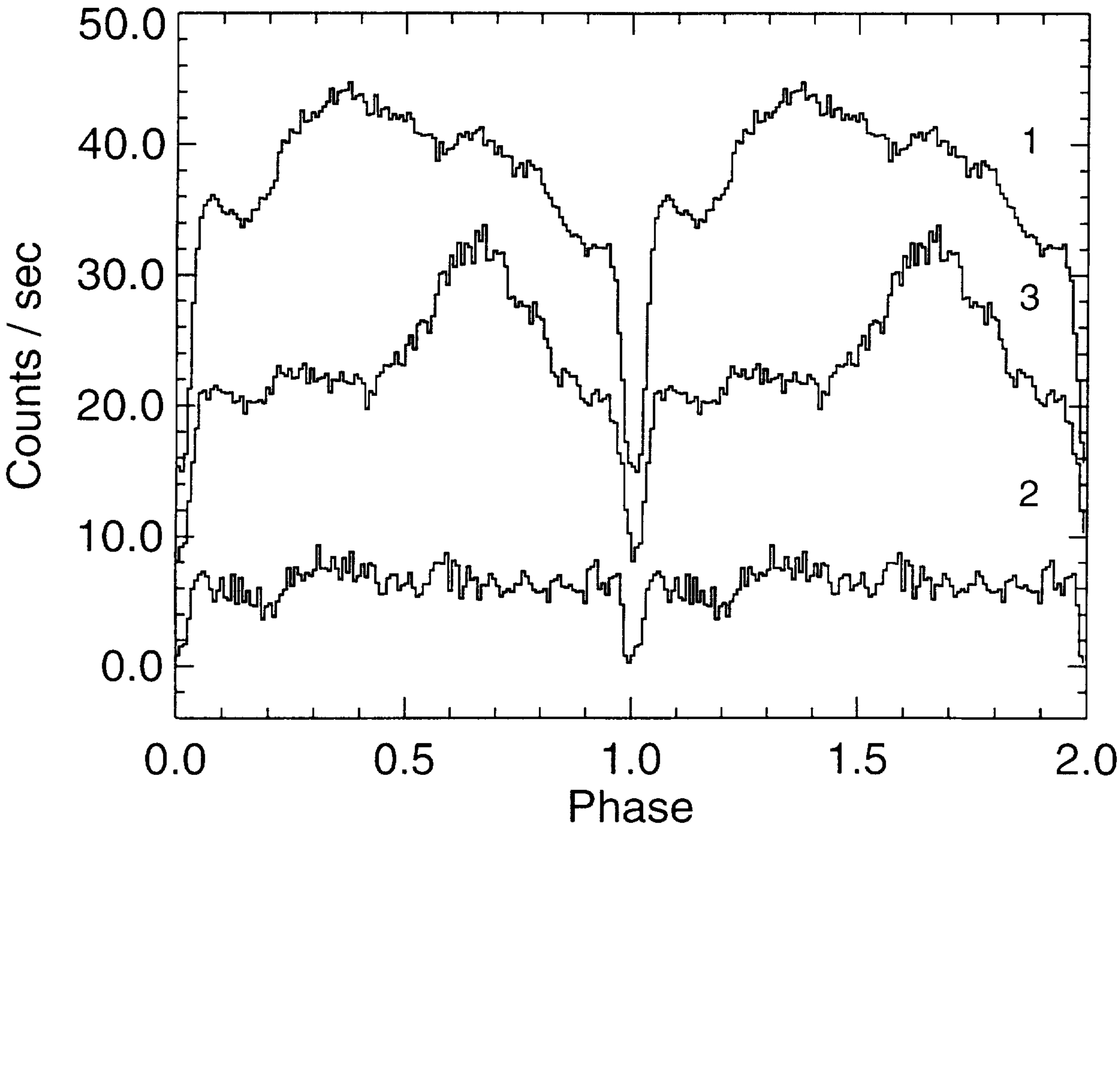
50.0
40.0
30.0
20.0
10.0
0.0
Counts / sec
1
3
2
0.0
0.5
1.0
1.5
2.0
Phase

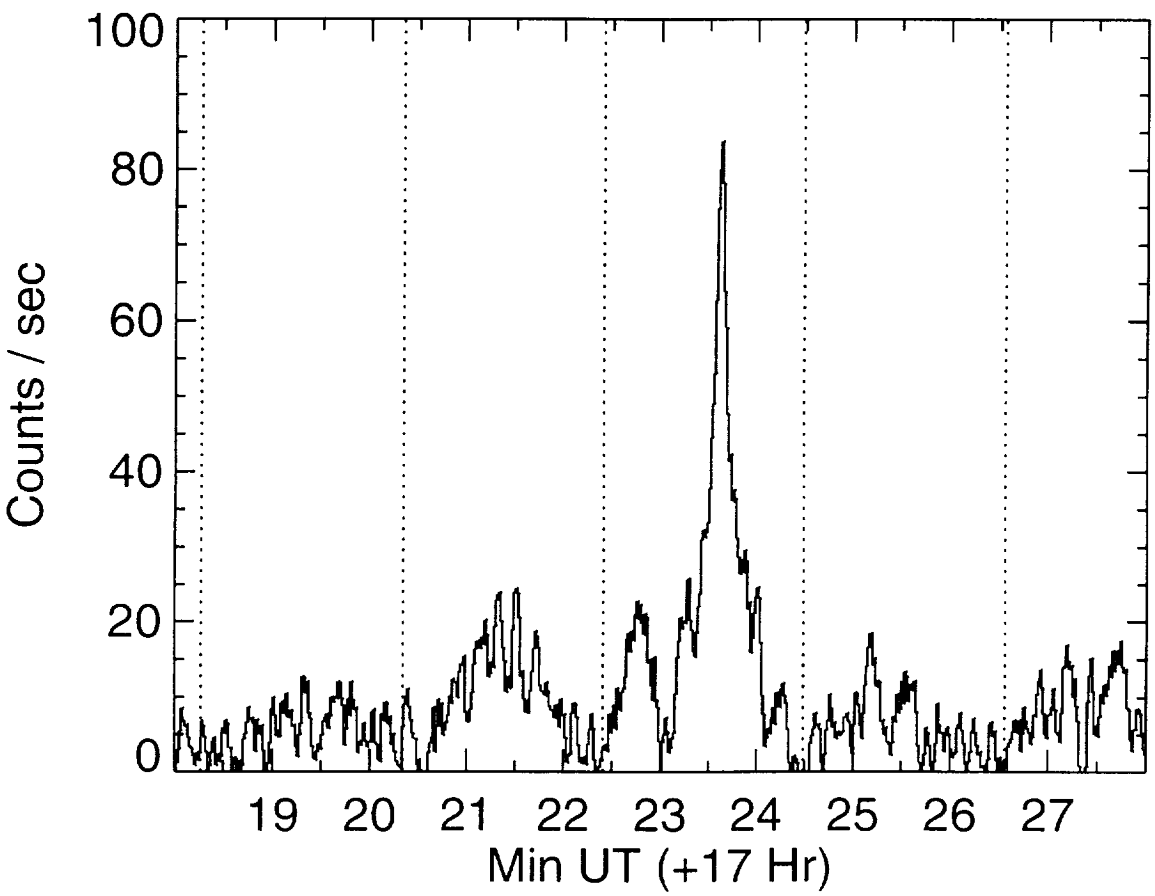

100
80
60
40
20
0
Counts / sec
19
20
21
22
23
24
25
26
27
Min UT (+17 Hr)